PLY RE-ORIENTATION IN COMPRESSION

R S JONES and R W ROBERTS

Department of Mathematics
University College of Wales
Aberystwyth, UK

1. Introduction

In the continuum theory of fibre-reinforced materials the constraint of inextensibility in the fibre direction imposes a severe limitation on the admissible deformations. Spencer [1] considered a material reinforced by two families of straight parallel fibres initially inclined at an angle 2ϕ to each other. He showed that in axial compression normal to the plane of the fibres, the fibres rotate until they are orthogonal whereupon no further contraction can take place. Thus there is a finite limit to the amount of contraction that can take place normal to the plane of the fibres and no contraction at all can take place if the fibres are initially orthogonal.

Many composites are made up of layers (plies) in which each ply consists of a single family of fibres and the fibre directions in alternate plies are inclined at an angle of 2ϕ to each other. Since the plies are thin the two family system could be thought of as a suitable model and the above deformation relevant. This was confirmed in an experiment carried out by Cogswell [2] who considered a stack of eleven plies, in the form of rhombi, in which fibres in alternate layers were initially inclined at $45°$ to each other. He found that under compression the angle tended towards $90°$.

In the present paper we present experimental results which extend the work of Cogswell using a fibre-reinforced composite in which the matrix (Golden Syrup) is liquid at room temperature. We also consider the theoretical model to take into account the interface conditions between the plies and between the plies and any resin-rich interply regions.

2. Experiment

The experiments were carried out using a model composite system consisting of carbon-fibre impregnated Golden Syrup supplied by ICI. This model composite has been shown [3] to have similar properties at room temperature to fibre-reinforced thermoplastics at their melt temperatures. Plies were cut into the shape of a rhombus of side 5cm and included angle $45°$ and laid up to form an N layer diamond such that the fibres in alternate layers were at $\pm 22\frac{1}{2}°$ to the axis through the points A, B (Fig 1).

The resulting laminate was compressed between two parallel perspex plates using a press. The experiment was carried out for different values of N. On removal from the press it was observed, in all cases, that the initial rhombus shape had tended towards a square with a shortening of the distance AB and an extension of CD. For instance, for $N = 5$, the length AB had contracted from its initial value of 9.3cm to 8.1cm and CD had increased from 3.8cm to 6.3cm. These observations are in agreement with those of Cogswell [2] who conducted a single experiment, on $APC - 2$ with 11 plies. There was also evidence of transverse flow normal to the fibres.
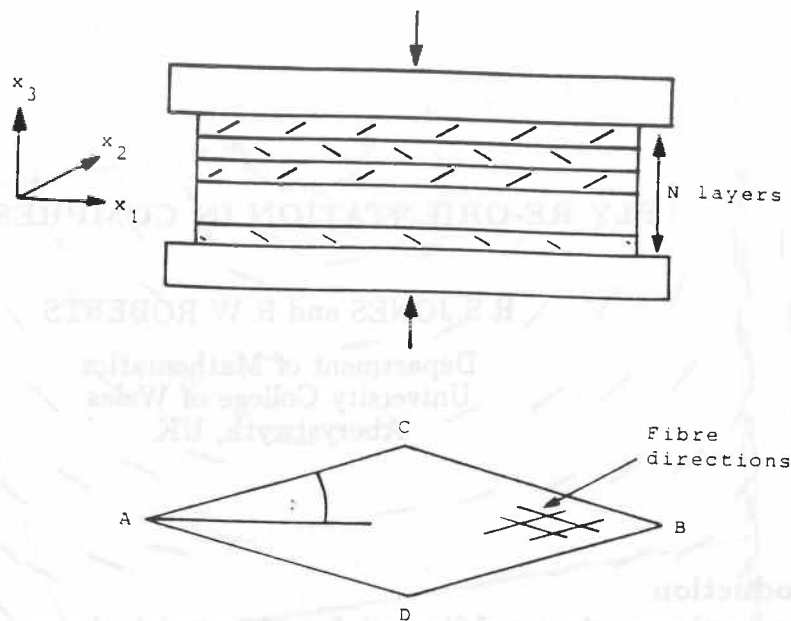
1

FIG 1.

The matrix was fluid at room temperature and so it was possible to peel the plies apart after removal from the press and record the angle ϕ between the axis AB and the fibre direction in each ply. These angles are given below in order from the top plate to the bottom for each value of N:

$N = 2$	24°	24°								
$N = 3$	24°	35°	24°							
$N = 4$	25°	37°	36°	24°						
$N = 5$	24°	40°	44°	40°	25°					
$N = 7$	24°	40°	42°	44°	43°	40°	25°			
$N = 9$	24°	40°	42°	38°	45°	40°	44°	42°	26°	
$N = 11$	23°	32°	40°	45°	43°	44°	44°	42°	41°	30°	26°

It is seen that the greatest rotation occurs in the centre plies and that the plies adjacent to the plates undergo little rotation. Some transverse flow normal to the fibre direction also took place.

A second series of experiments was carried out in which a thin layer of the Golden Syrup matrix was introduced between each ply and between the plies and the plates. After compression the structure was examined and the angle ϕ measured for each ply as before. The results were as follows:

$N = 2$	44°	45°						
$N = 3$	44°	45°	44°					
$N = 4$	44°	45°	45°	43°				
$N = 8$	40°	45°	45°	45°	45°	45°	45°	40°

It is seen that the effect of introducing the viscous layer is to enhance the rotation. In the case of two plies it could be seen, through the perspex plates, that the deformation consisted of an initial rotation of the fibres until a square shape was formed followed by lateral spreading normal to the sides of the square. Further compression resulted in the phenomena of 'barrelling' and 'jetting' which have also been observed for $APC - 2$ under high pressures [4]. This deformation sequence is illustrated in Fig 2.

2

Rotation | Transverse flow
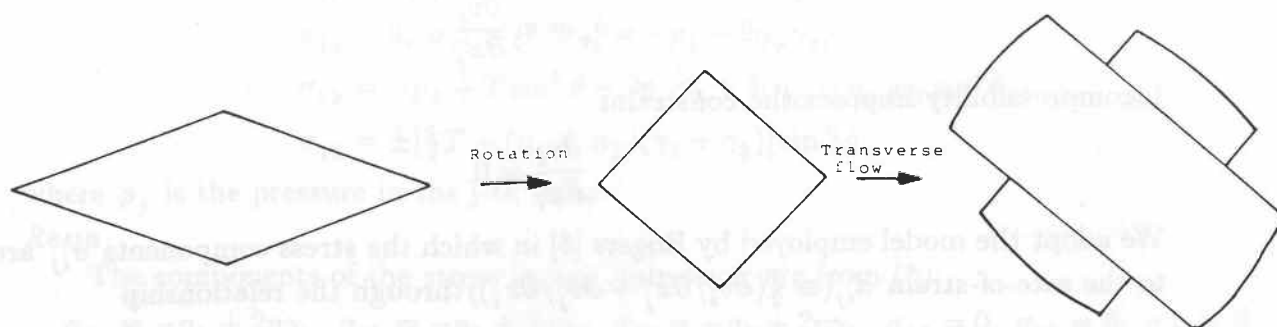
FIG 2.

The enhancement of the rotation and the subsequent transverse flow suggested that the introduction of a resin rich layer could induce an extensional flow which might have beneficial effects in a manufacturing process. Two rectangular samples were made in which the fibres were given a wave form and subjected to normal pressure. In one case resin-rich layers were introduced between the sample and the plates and it was seen that the fibres initially straightened before a transverse flow took place. In the non-lubricated case the fibres remained wavy in form.

3. Theoretical Model

We consider the composite to be modelled as a stack of N layers contained between parallel plates which approach each other with a speed V. Cartesian axes are chosen with the x_3−axis normal to the plates and the fibres in each ply are assumed to lie in planes normal to the x_3−axis. We allow the possibility that the plies are separated by resin-rich layers. The configuration is illustrated in Fig 1.

The normal motion of the plates will induce velocity and stress fields in each layer which in general will be functions of position and time. The problem is one of finding a velocity distribution that satisfies the constitutive equations and the equations of motion in each layer together with the interface conditions between the layers. The latter requires continuity of velocity and continuity of shear and normal stress. There will also be edge conditions which we take to be zero in-plane shear stress and a global equilibrium condition on the normal stress.

3.1 Constitutive Equations

Plies

The plies are modelled as a highly anisotropic viscous fluid [5]. The material is not only incompressible but inextensible in the fibre direction. The local fibre direction at any point is denoted by a unit vector a with components $a_i (i = 1, 2, 3)$ where $a_i a_i = 1$. Inextensibility in the fibre direction imposes the constraint

$$a_i a_j \frac{\partial v_i}{\partial x_j} = 0,$$

(1)

3

where v_i are the components of the velocity vector $\boldsymbol{v}$, and it can also be shown [1] that the material time derivative of $\boldsymbol{a}$ has components

$$\dot{a}_i = a_j \frac{\partial v_i}{\partial x_j}.$$

(2)

Incompressibility imposes the constraint

$$\frac{\partial v_i}{\partial x_i} = 0.$$

(3)

We adopt the model employed by Rogers [6] in which the stress components σ_{ij} are related to the rate-of-strain $d_{ij} (\equiv \frac{1}{2}(\partial v_i/\partial x_j + \partial v_j/\partial x_i))$ through the relationship

$$\sigma_{ij} = -p\delta_{ij} + Ta_i a_j + 2\eta_T d_{ij} + 2(\eta_L - \eta_T)(a_i a_k d_{kj} + a_j a_k d_{ik}),$$

(4)

where p is the pressure, T is an arbitrary tension arising from the constraint of inextensibility, and η_L, η_T are the shear viscosities along and transverse to the fibre directions.

Resin layers

The resin layers are modelled as incompressible viscous fluids of constant viscosity η for which

$$\sigma_{ij} = -p\delta_{ij} + 2\eta d_{ij}.$$

(5)

3.2 Equations of Motion

We assume that both the resin layers and the plies are sufficiently viscous and that the flow is sufficiently slow for inertia to be neglected. The stress equations of motion are then

$$\frac{\partial \sigma_{ij}}{\partial x_j} = 0.$$

(6)

The motion is therefore quasi-static with time entering only through the boundary conditions. We seek solutions for which the interfaces between the layers remain plane for all times and in which the fibres in any one ply remain straight and parallel in planes normal to the x_3−axis. In the present paper we limit our attention to two basic flows of this type, uniform extensional flows and squeezing flows.

3.3 Uniform Extensional Flows

This deformation has been considered in some detail by Spencer [1] for the homogeneous case with both one and two families of fibres. The trivial extension to the layered system is included here since it demonstrates a mechanism for the rotation that may be valid far from the boundaries. Consider a deformation in which the velocity distribution in the jth layer is of the form $v_i^{(j)} = \gamma_i^{(j)} x_i$, $(i = 1, 2, 3)$, where the $\gamma_i^{(j)}$ are functions of time. On every interface, $x_3 = g^{(j)}(t)$, the velocity must be continuous and it follows that the $\gamma_i^{(j)}$ must be the same for each layer and we can write $\gamma_i^{(j)} = \gamma_i$.

Plies

We suppose that the plies in alternate layers are inclined at an angle 2θ and choose the x_1−axis to bisect this angle. Then in any ply the vector $\boldsymbol{a} = (\cos\theta, \pm\sin\theta, 0)$ and equations (3), (1) and (2) give

$$\gamma_1 + \gamma_2 + \gamma_3 = 0, \qquad \gamma_1 \cos^2\theta + \gamma_2 \sin^2\theta = 0,$$
$$-\sin\theta\dot{\theta} = \gamma_1 \cos\theta, \qquad \cos\theta\dot{\theta} = \gamma_2 \sin\theta.$$

(7)

It follows that

$$\dot{\theta} = -\gamma_3 \tan 2\theta.$$

(8)

4

The components of stress are, from (4),

$$\sigma_{11} = -p_j + T\cos^2\theta + 2\eta_T\gamma_1 + 4(\eta_L - \eta_T)\gamma_1\cos^2\theta,$$

$$\sigma_{13} = 0, \ \sigma_{23} = 0, \ \sigma_{33} = -p_j + 2\eta_T\gamma_3,$$

$$\sigma_{22} = -p_j + T\sin^2\theta + 2\eta_T\gamma_2 + 4(\eta_L - \eta_T)\gamma_2\sin^2\theta,$$

$$\sigma_{12} = \pm[\tfrac{1}{2}T + (\eta_L - \eta_T)(\gamma_1 + \gamma_2)]\sin 2\phi$$

where p_j is the pressure in the j-th layer.

Resin

The components of the stress in any resin layer are from (5):

$$\sigma_{11} = -p_k + 2\eta\gamma_1, \ \sigma_{22} = -p_k + 2\eta\gamma_2, \ \sigma_{33} = -p_k + 2\eta\gamma_3, \ \sigma_{12} = 0, \ \sigma_{13} = 0, \ \sigma_{23} = 0,$$

where p_k is the pressure in the k-th layer.

Both of these stress fields satisfy the equations of motion (6) identically. At any interface we require continuity of the stress components σ_{13}, σ_{23} and σ_{33}. It is clear that this can always be accomplished by a suitable choice of the pressures p_j, p_k. In a compressive flow $\gamma_3 < 0$, and it follows from (7) and (8) that if θ is initially less than $\pi/4$ it will increase to $\pi/4$ where γ_3 must be zero, and no further contraction can take place. Since the γ_i do not depend on x_3 the positions of the interfaces are arbitrary, and we cannot satisfy the boundary and edge conditions so that the deformation can only be expected to hold, if at all, far from the boundaries. It is perhaps significant that in the experiments the greatest rotation occurred in the centre plies. It is also noteworthy that in the experiments the material did not 'lock' and subsequent to the rotation transverse flow did take place.

3.4 Squeezing flows

In the experiments it was observed that in addition to the fibre rotation there was also some transverse flow normal to the fibres. In the case of the lubricated samples there was an initial rotation until the fibres were orthogonal followed by a transverse flow. Such a deformation is not allowed under the uniform extension considered above. It is of interest therefore to consider the deformation that takes place when the plies in alternate layers are orthogonal. As before we allow the possibility of inter-ply resin-rich layers.

Plies

The squeezing flow of a single ply between parallel plates has been considered by Rogers [6] and Balasubramanyam et al [7] and we shall make use of these solutions in what follows; the reader is referred to the original papers for the details. Consider a single ply in which the fibres are initially straight and parallel to the x_2-axis. It has been shown that a possible velocity field is $v_1 = -f'(x_3, t)x_1$, $v_2 = 0$, $v_3 = f(x_3, t)$ where a dash indicates differentiation with respect to x_3. It follows from (2) that $\dot{a}_i = 0$; that is, the fibres remain straight and parallel to the x_2-axis. The components of stress are, using (4),

$$\sigma_{11} = -p - 2\eta_T f', \ \sigma_{22} = -p + T, \ \sigma_{33} = -p + 2\eta_T f', \ \sigma_{13} = -\eta_T x_1 f'', \ \sigma_{23} = \sigma_{12} = 0.$$

The equations of motion then become

$$\frac{\partial p}{\partial x_1} = -\eta_T f''', \quad \frac{\partial}{\partial x_2}(-p + T) = 0, \quad \frac{\partial p}{\partial x_3} = \eta_T f''. \tag{9}$$

For consistency

$$f = Ax_3^3 + Bx_3^2 + Cx_3 + D, \tag{10}$$

where the coefficients are functions of time, and

$$p = p_0 + \eta_T\{3Ax_3^2 + 2Bx_3 + C - 3Ax_1^2\} + g(x_2, t), \tag{11}$$

5

where p_0 is an arbitrary function of time and g is an arbitrary function of x_2 and t. The presence of the function g is due to the fact that in the second of the equations in (9) only the combination $(-p+T)$ arises, so we may add on to p any function of x_2 and t provided we subtract it from T. This point has not been considered in previus work but it has the important consequence that if any resin flow in the x_2-direction creates a tension that depends on x_2, it will affect the pressure and hence any calculation relating to the normal load on the plates. For the present work this additional function is essential when we come to the interface conditions.

3.5 <u>Example 1 - two plies ($0 - 90°$ lay-up)</u>

In order to illustrate the interface conditions it is useful to consider the case of two plies in a 0-90° lay-up with no resin-rich interply regions. The configuration is illustrated in Fig 3:
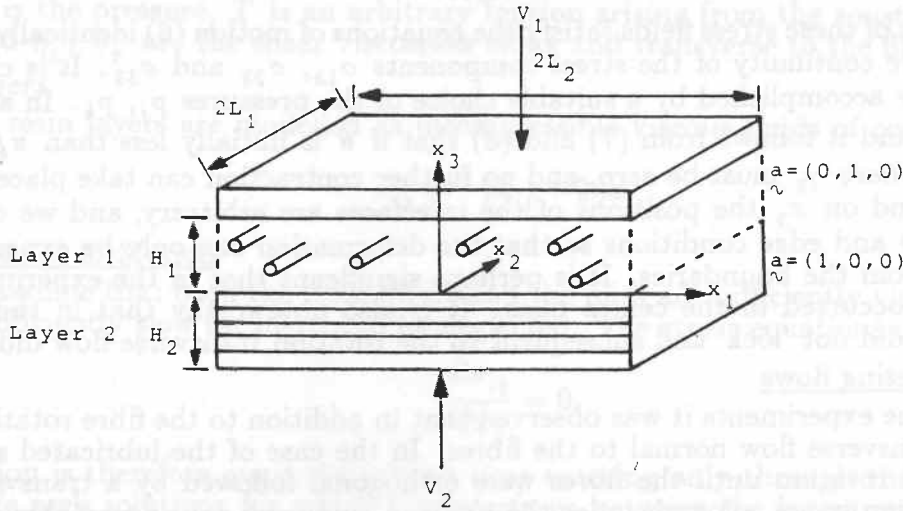
FIG 3.

We choose an origin in the interface which is taken to be at rest and the top and bottom plates approach with speeds V_1 and V_2 respectively. Using the above solution we have for layer 1:

$$v_1^{(1)} = -f_1'(x_3)x_1, \quad v_2^{(1)} = 0, \quad v_3^{(1)} = f_1(x_3), \qquad (12)$$

where $f_1 = A_1 x_3^3 + B_1 x_3^2 + C_1 x_3 + D_1$. The boundary conditions on the top plate require:

$$v_1^{(1)} = 0, \quad v_3^{(1)} = -V_1 \quad \text{on} \quad x_3 = H_1. \qquad (13)$$

For layer 2,

$$v_1^{(2)} = 0, \quad v_2^{(2)} = -f_2'(x_3)x_2, \quad v_3^{(2)} = f_2(x_3), \qquad (14)$$

where

$$f_2 = A_2 x_3^3 + B_2 x_3^2 + C_2 x_3 + D_2,$$

and

$$v_2^{(2)} = 0, \quad v_3^{(2)} = V_2 \quad \text{on} \quad x_3 = -H_2.$$

6

Interface conditions

On the interface, $x_3 = 0$, we require:

(a) Continuity of velocity, i.e.

$$\left.\begin{array}{l} v_1^{(1)} = v_1^{(2)} = 0 \text{ which implies } C_1 = 0, \\[2mm] v_2^{(2)} = v_2^{(1)} = 0 \text{ which implies } C_2 = 0, \\[2mm] v_3^{(1)} = v_3^{(2)} = 0 \text{ which implies } D_1 = D_2 = 0. \end{array}\right\} \tag{15}$$

(b) Continuity of normal stress σ_{33}, i.e.

$$-p_0^{(1)} + \eta_T 3A_1 x_1^2 - g_1(x_2, t) = -p_0^{(2)} + \eta_T 3A_2 x_2^2 - g_2(x_1, t), \tag{16}$$

and we see that we must choose

$$g_1 = -\eta_T 3A_2 x_2^2 \text{ and } g_2 = -\eta_T 3A_1 x_1^2.$$

(c) Continuity of shear stress

$$\sigma_{13}^{(1)} = \sigma_{13}^{(2)}, \quad \sigma_{23}^{(1)} = \sigma_{23}^{(2)}, \quad \text{on} \quad x_3 = 0. \tag{17}$$

Now $\sigma_{31}^{(1)} = -\eta_T B_1 x_1$ and $\sigma_{13}^{(2)} = 0$, so either $B_1 = 0$ or we must allow a discontinuity in the shear stress. Similarly $\sigma_{23}^{(1)} = \sigma_{23}^{(2)}$ implies either $B_2 = 0$ or that there is a discontinuity in the shear stress. If $B_1 = B_2 = 0$ then it follows from the boundary conditions (13) and (14) that $V_1 = V_2 = 0$ and no flow is possible. However, for region (2), consider the fibres at the interface, these have zero shear stress on them from below and a constant shear stress $\sigma_{31}^{(1)}$ from above. We may write

$$\sigma_{31}^{(2)} = \sigma_{31}^{(1)}(0)(1 - H(x_3)),$$

where $H(x_3)$ is the unit step function. The stress equations of motion require

$$\frac{\partial \sigma_{11}^{(2)}}{\partial x_1} + \frac{\partial \sigma_{13}^{(2)}}{\partial x_3} = 0,$$

which integrate to give

$$\sigma_{11}^{(2)} = -\frac{B_1 \eta_T}{2}(x_1^2 - L_1^2)\delta(x_3),$$

where $\delta(x_3)$ is the Dirac delta function. Thus the tensile stress becomes infinite in the boundary fibres which carry a finite force $F_2 = -\eta_T B_1 (x_1^2 - L_1^2)/2$. This is an example of a singular fibre which have been examined in some detail in the literature for fibre reinforced solids [8]. Note that the interface is plane so that there is no singularity in the pressure. In a similar manner we can see that for region 1, $x_3 > 0$, the shear stress $\sigma_{23}^{(1)}$ is discontinuous and the boundary fibres carry a finite force $-\eta_T B_2(x_2^2 - L_2^2)/2$. Thus the inextensibility of the fibres and their ability to carry a finite force ensures that condition (17) is satisfied.

Edge conditions

Zero traction on the two edges perpendicular to the fibre direction requires

$$\sigma_{22}^{(1)} = 0 \quad \text{on} \quad x_1 = \pm L_1.$$

$$\sigma_{11}^{(2)} = 0 \quad \text{on} \quad x_2 = \pm L_2.$$

Global equilibrium of the edge region is satisfied if

$$\int_{-L_2}^{L_2} \int_0^{H_1} \sigma_{11}^{(1)} \bigg|_{x_1 = \pm L_1} dx_3 dx_2 = 0 \quad \text{and} \quad \int_{-L_1}^{L_1} \int_{-H_2}^0 \sigma_{22}^{(2)} \bigg|_{x_2 = \pm L_2} dx_3 dx_1 = 0.$$

These relate the two pressures $p_0^{(1)}$ and $p_0^{(2)}$ to the A's and B's:

$$p_0^{(1)} = 3\eta_T [(A_1 + \tfrac{1}{3} A_2)L_1^2 - (A_1 H_1^2 + B_1 H_1)], \tag{18}$$

$$p_0^{(2)} = 3\eta_T [(A_2 + \tfrac{1}{3} A_1)L_2^2 - (A_2 H_2^2 + B_2 H_2)]. \tag{19}$$

The set of algebraic equations (13)-(19) for the A's and B's can now be solved to give

$$v_1^{(1)} = 6\frac{V_1 x_3(-x_3 + H_1)x_1}{H_1^3}, \quad v_2^{(1)} = 0, \quad v_3^{(1)} = -\frac{V_1 x_3^2(3H_1 - 2x_3)}{H_1^3},$$

$$v_1^{(2)} = 0, \quad v_2^{(2)} = -\frac{6V_2}{H_2^3}x_3(x_3 + H_2)x_2, \quad v_3^{(2)} = \frac{V_2 x_3^2(2x_3 + 3H_2)}{H_2^3}$$

where

$$V_2 = \frac{V_1(6L_2^2 + 3H_1^2 - 2L_1^2)H_2^3}{H_1^3(6L_1^2 + 3H_2^2 - 2L_2^2)}.$$

This solution is of interest in that a plane interface is possible. This is not the case for two Newtonian fluids where the interface and edge conditions can only be satisfied approximately if further assumptions such as the lubrication approximation are made.

3.6 Example 2 - five layers

We now extend the above analysis to the case where resin rich layers exist between the plies and between the plies and the plates. We also assume a constant load F on the top and bottom plates so that V, H_1, H_2 and H_3 are functions of time to be determined. The configuration is one of five layers as depicted in Fig 4.

For simplicity we assume that the layers are square in section so that $-L \le x_i \le L$, $(i = 1, 2)$, with the interfaces at $x_3 = \pm H_1$, $x_3 = \pm H_2$ and the boundaries at $x_3 = \pm H_3$. In each of the resin layers, i.e. layers 1, 3, 5, we assume a velocity field of the form

$$v_1^{(i)} = -g_1^{(i)\prime} x_1 - g_2^{(i)\prime} x_2, \quad v_2^{(i)} = -g_3^{(i)\prime} x_2 - g_4^{(i)\prime} x_1, \quad v_3^{(i)} = g_1^{(i)} + g_3^{(i)}, \quad (i = 1, 2, 3)$$

where the g's are functions of x_3 and time and a dash denotes differentiation with respect to x_3. These satisfy continuity and from the equations of motion for each layer it can be deduced that

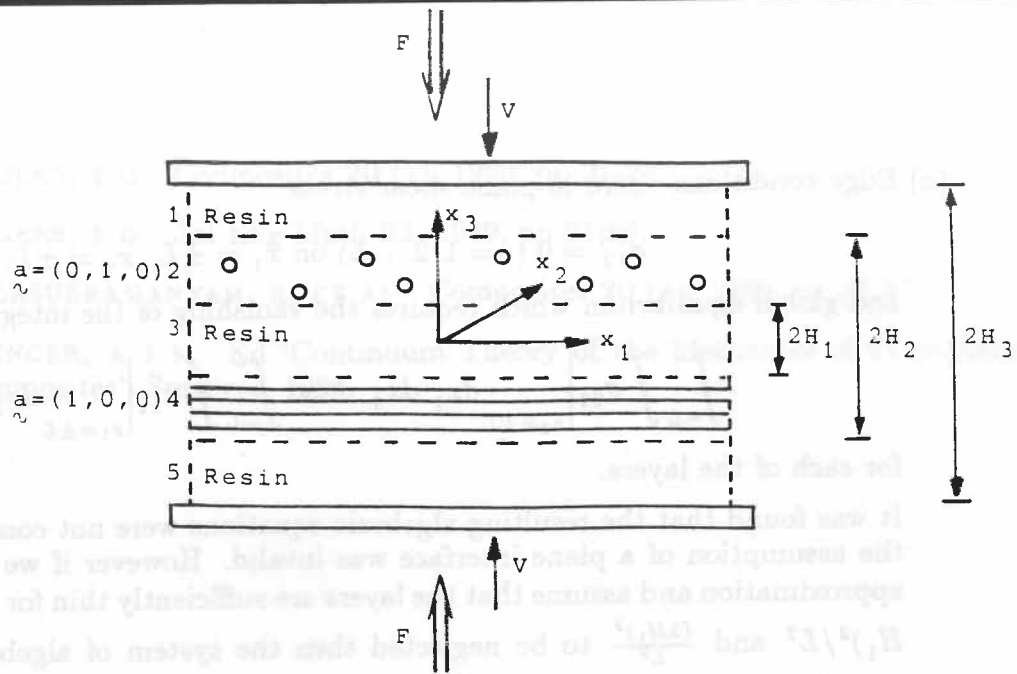$$g_N^{(i)} = a_N^{(i)} x_3^3 + b_N^{(i)} x_3^2 + c_N^{(i)} x_3 + d_N^{(i)}, \quad (i = 1, 3, 5)(N = 1, 2, 3, 4).$$

8

FIG 4.

The velocity fields in the two plies have the same form as in the previous example, i.e.

$$v_1^{(2)} = -g_1^{(2)'} x_1, \quad v_2^{(2)} = 0, \quad v_3^{(2)} = g_1^{(2)},$$
$$v_1^{(4)} = 0, \quad v_2^{(4)} = -g_3^{(4)'} x_2, \quad v_3^{(4)} = g_3^{(4)},$$

where

$$g_N^{(i)} = a_N^{(i)} x_3^3 + b_N^{(i)} x_3^2 + c_N^{(i)} x_3 + d_N^{(i)} \quad (i = 2, \ N = 1)(i = 4, \ N = 3).$$

It is now necessary to determine the 56 coefficients $a_N^{(i)}$, $b_N^{(i)}$, $c_N^{(i)}$, $d_N^{(i)}$ from the boundary conditions, interface conditions and the edge conditions. These are

(a) Boundary conditions - no-slip and continuity of normal velocity:

$$v_1^{(1)} = v_2^{(1)} = 0, \quad v_3^{(1)} = -V, \quad \text{on} \quad x_3 = H_3$$

and from symmetry $v_3^{(3)} = 0$ on $x_3 = 0$.

(b) Interface conditions - continuity of velocity and normal and shear stresses:

$$v^{(1)}(H_2) = v^{(2)}(H_2), \ v^{(3)}(H_1) = v^{(2)}(H_1), \ v^{(3)}(-H_1) = v^{(4)}(-H_1), \ v^{(4)}(-H_2) = v^{(5)}(-H_2);$$

$$\sigma_{33}^{(1)}(H_2) = \sigma_{33}^{(2)}(H_2), \ etc,$$

$$\sigma_{13}^{(1)}(H_2) = \sigma_{13}^{(2)}(H_2), \ \sigma_{13}^{(2)}(H_1) = \sigma_{13}^{(3)}(H_1),$$

$$\sigma_{23}^{(3)}(-H_1) = \sigma_{23}^{(4)}(-H_1), \ \sigma_{23}^{(4)}(-H_2) = \sigma_{23}^{(5)}(-H_2).$$

Note that we need only impose continuity of the shear stress σ_{13} on the surfaces $x_3 = H_2$ and $x_3 = H_1$ since the component σ_{32} is accommodated by the tension in the surface fibres in layer 2. Similarly on $x_3 = -H_1$ and $x_3 = -H_2$ we need only impose continuity of σ_{23}.

9

(c) Edge conditions - zero in-plane shear stress

$$\sigma_{12}^{(i)} = 0 \ (i = 1, 2 \ldots 5) \text{ on } x_1 = \pm L, \ x_2 = \pm L,$$

and global equilibrium which requires the vanishing of the integrals

$$\int_{-L}^{L} \int \sigma_{22}\bigg|_{x_2 = \pm L} dx_1 \, dx_3 \quad \text{and} \quad \int_{-L}^{L} \int \sigma_{11}\bigg|_{x_1 = \pm L} dx_2 \, dx_3$$

for each of the layers.

It was found that the resulting algebraic equations were not consistent indicating that the assumption of a plane interface was invalid. However if we adopt the lubrication approximation and assume that the layers are sufficiently thin for $(H_3 - H_2)^2/L^2$, $(H_2 - H_1)^2/L^2$ and $\frac{(2H_1)^2}{L^2}$ to be neglected then the system of algebraic equations can be solved to give the velocities $v_j^{(i)}$ in terms of V, H_1, H_2 and H_3. These are then related to the given load F through

$$F = \int_{-L}^{L} \int_{-L}^{L} p^{(1)} dx_1 dx_2.$$

Finally H_1, H_2 and H_3 were obtained as functions of time by integrating the resulting coupled equations for $\dot{H}_1$, $\dot{H}_2$ and $\dot{H}_3$. This was accomplished using the algebraic package MAPLE.

Graphs of the height profiles are shown in figures 5, 7, 9 and 11 for different viscosities η, η_T and initial thicknesses $H_3^0 - H_2^0$, $H_2^0 - H_1^0$, $2H_1^0$.

Similarly graphs of the corresponding velocity profiles through the laminate thickness are shown in figures 6, 8, 10 and 12. Note that the profiles in regions 4 and 5 are the same as those for regions 1 and 2 in the x_2-direction so that each figure contains complete information about the velocity profiles v_1, v_2 for each layer.

From these figures it can be observed that

(i) large values of η_T induces plug flow in the plies (Figs 8,12);

(ii) thin resin layers persist and push out the ply layers which thin more rapidly (Fig 10);

(iii) with equal initial thicknesses of resin and ply layers the maximum speed can occur in the resin regions (Figs 6,8).

References

[1] SPENCER, A J M 'Deformations of Fibre-reinforced Materials', Oxford, 1972.

[2] COGSWELL, F N Private communication.

[3] WHEELER, A B PhD thesis University of Wales, 1989.

[4] BARNES, J Private communcation.

[5]   ROGERS, T G   Composites **20** (1), 1989, pp 21-28.

[6]   ROGERS, T G   Jnl Eng Math **23**, 1989, pp 21-89.

[7]   BALASUBRAMANYAM, R, ET AL   Composites **20** (1), 1989, pp 33-37.

[8]   SPENCER, A J M   Ed 'Continuum Theory of the Mechanics of Fibre-Reinforced Composites', Springer, 1984.
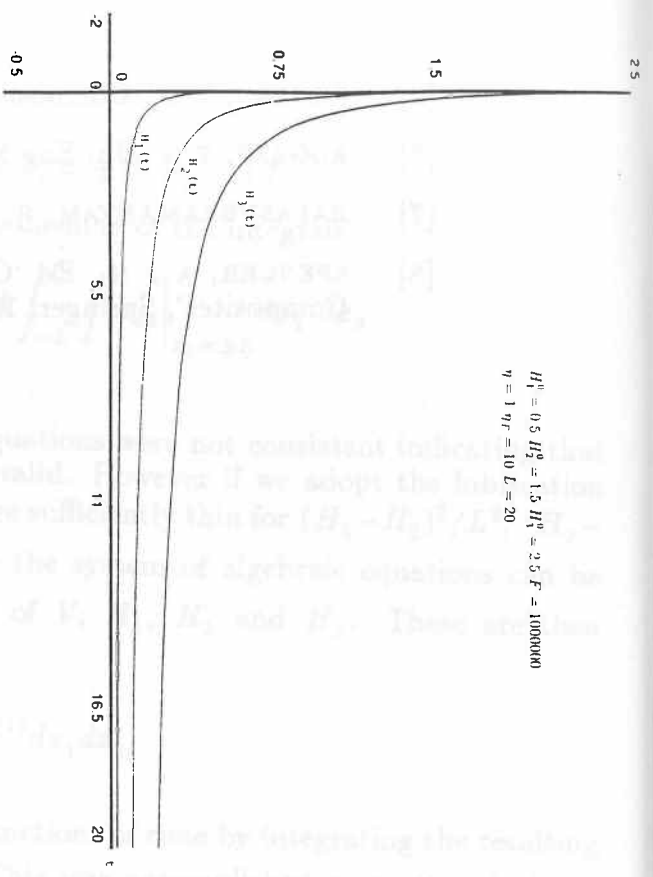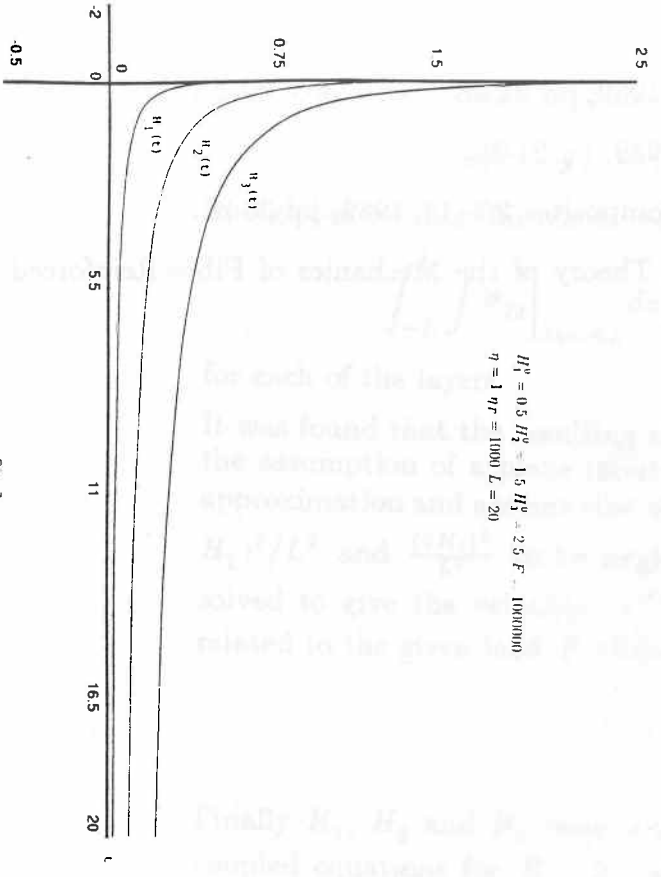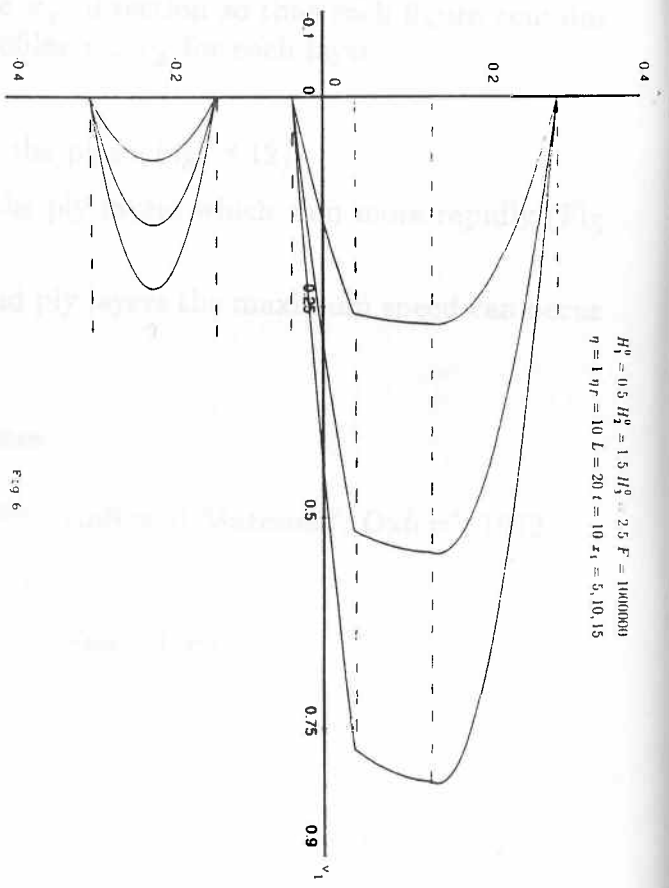
for each of the layers.
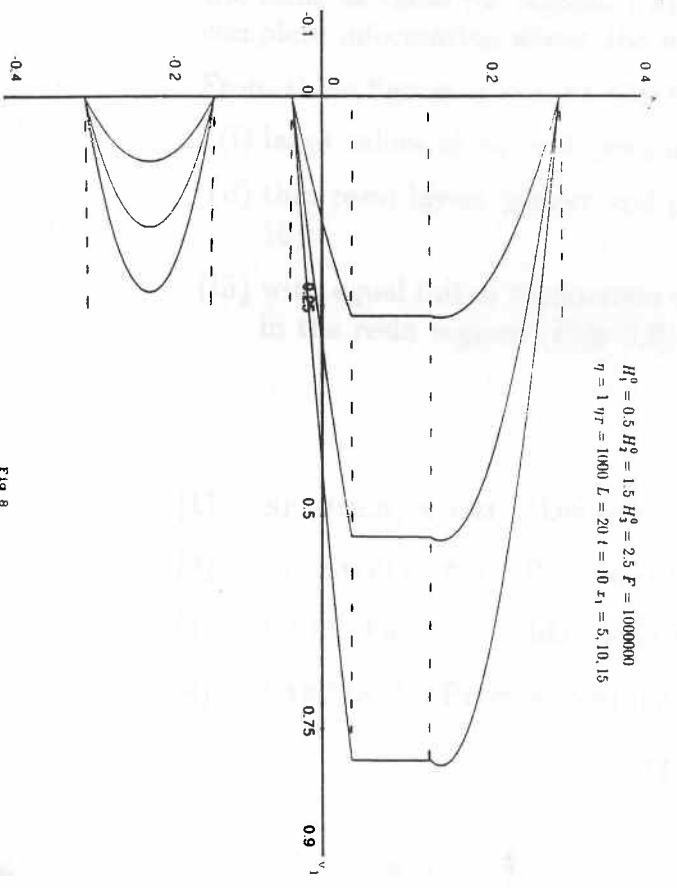
It was found that the resulting algebraic equations were not consistent indicating that the assumption of a plane interface was invalid. However if we adopt the lubrication approximation and assume also the layers are sufficiently thin for $(H_1 - H_2)^2/L^2$, $H_1'^3/L^3$ and $\frac{\partial^2 H_1}{\partial x^2}$ are neglected then the system of algebraic equations can be solved to give the velocity $v^{(i)}$ in terms of V_i, H_1, H_2 and H_3. These are also related to the given load F through

$$\int \int p^{(i)} dx_1 dx_2$$

Finally H_1, H_2 and H_3 were obtained as functions of time by integrating the resulting coupled equations for H_1, H_2 and H_3. This was accomplished using the algebraic package MAPLE.

Graphs of the height profiles are shown in figures 6, 7, 9 and 11 for different viscosities η, η_T and initial thicknesses $H_2^0 - H_2^0$, $H_3^0 - H_1^0$, $2H_1^0$.

Similarly graphs of the average-acting velocity profiles through the laminate thickness are shown in figures 5, 6, 10 and 12. Note that the profiles at regions 4 and 5 are the same as those for regions 1 and 2 in the x_2 direction so the graph 8 etc contains complete information about the velocity profiles for each layer.

Fig 5

Fig 6

Fig 7

Fig 8

References

[1]

[5]

[6]

[7]

[8]

Fig 9

$$H_1^0 = 0.05 \quad H_2^0 = 1.1 \quad H_3^0 = 1.2 \quad F = 1000000$$
$$\eta = 1 \quad \eta_T = 10 \quad L = 20$$

Fig 10

$$H_1^0 = 0.05 \quad H_2^0 = 1.1 \quad H_3^0 = 1.2 \quad F = 1000000$$
$$\eta = 1 \quad \eta_T = 10 \quad L = 20 \quad t = 20 \quad z_1 = 5, 10, 15$$

Fig 11

$$H_1^0 = 0.05 \quad H_2^0 = 1.1 \quad H_3^0 = 1.2 \quad F = 1000000$$
$$\eta = 1 \quad \eta_T = 1000 \quad L = 20$$

Fig 12

$$H_1^0 = 0.05 \quad H_2^0 = 1.1 \quad H_3^0 = 1.2 \quad F = 1000000$$
$$\eta = 1 \quad \eta_T = 1000 \quad L = 20 \quad t = 20 \quad z_1 = 5, 10, 15$$